A Fused Poly(truncated rhombic dodecahedron)-Containing 3D Coordination Polymer: A Multifunctional Material with Exceptional Properties

Adrien Schlachter, Kevin Tanner, Rebecca Scheel, Paul-Ludovic Karsenti, Carsten Strohmann, Michael Knorr, Pierre Harvey

A Fused Poly(truncated rhombic dodecahedron)-containing 3D-Coordination Polymer: A Multifunctional Material With Exceptional Properties

Adrien Schlachter,[†] Kevin Tanner,[†] Rebecca Scheel,[§] Paul-Ludovic Karsenti,[†] Carsten Strohmann,[§] Michael Knorr[,‡] and Pierre D. Harvey*[,†]*

†Département de Chimie, Université de Sherbrooke 2550 Boulevard Université, Sherbrooke, PQ, Canada, J1K 2R1.

‡Institut UTINAM, UMR CNRS 6213, Université Bourgogne Franche-Comté, 16, Route de Gray, 25030 Besançon, France.

§Anorganische Chemie, Technische Universität Dortmund, Otto-Hahn-Straße 6, 44227 Dortmund, Germany.

KEYWORDS. Coordination polymer ; thermochromism ; templated solid-state synthesis ; near-IR phosphor ; solid-to-solid phase transition

ABSTRACT

The design of new and inexpensive metal-containing functional materials is of great interest. Herein is reported a unique thermochromic near-IR emitting coordination polymer, 3D-$[Cu_8I_8(\mathbf{L1})_2]_n$, **CP2**, which is formed when $ArS(CH_2)_4SAr$ (**L1**, Ar = 4-C_6H_4OMe) reacts with 2 eq. of CuI in EtCN. In MeCN, **CP1** ($[Cu_4I_4(\mathbf{L1})(MeCN)_2]_n$, consisting of an alternating [-Cu_4I_4-**L1**-Cu_4I_4-**L1**-]$_n$ chain where the Cu_4I_4 cubane units bears two metal-bound MeCN molecules, is formed. Heat-driven elimination of these MeCN's in solid **CP1** also leads to **CP2** through a predisposed organisation of the Cu_4I_4 units prone to fusion after MeCN eliminations (*i.e*. a rare case of template effect). The **CP2** structure exhibits parallel 1D-$(Cu_8I_8)_n$ chains, (*z*-axis; designated 1D-$[CuI]_n$) as secondary building units (SBU) held together by parallel thioether ligands (*x*,*y*-axes) forming a non-porous 3D-network. The structure of this1D-$[CuI]_n$ SBU is unprecedented and consists of a series of fused and twisted open Cu_4I_4 cubanes forming a fused poly(truncated rhombic dodecahedron). Unexpectedly, the compact 3D **CP2** exhibits a solid-to-solid phase transition at 100°C and a hysteresis of ~20 °C. **CP1** emits intensively (298K: λ_{emi} = 564 nm; Φ_e = 0.35) while **CP2** presents a strongly red-shifted weaker emission (298K: λ_{emi} ~ 740 nm, Φ_e < 0.0001). Moreover, **CP2**, which is stable over long periods of time, exhibits thermochromism where the emission intensity of the near-IR band decreases significantly at the benefit of a ligand-centred phosphorescence at 415 nm. Altogether these properties listed above makes **CP2** exceptional. The low-energy singlet and triplet excited states have been assigned to ligand/metal-to-ligand charge transfer based on DFT and TD-DFT computations.

INTRODUCTION

Since the early investigations on the strongly luminescent closed $Cu_4I_4L_4$ cubanes (L = *N*- and *P*-donors),[1] a tremendous interest among researchers in quest of new functional, stimuli-responsive and smart materials, has emerged.[2–4] This interest included $Cu_4X_4L_4$ species (X = OH) as well.[5] Nowadays, the design of new materials focusses on introducing this motif or higher-nuclear derivatives (*i.e.* $Cu_xX_xL_y$; X = Cl, Br, I; x = 2-8; 4 < y <8) inside 1D-, 2D-, and 3D-coordination polymers through the use of bi- and polydentate ligands. In parallel, the replacement of the *N*- and *P*-donor homo-ligands by chalcogenoethers (literature reveals that the *S*-donor ligands are the most reported) also leads to 1D-, 2D-, and 3D-coordination polymers.[6–9] From these networks, a large range of applications have emanated including luminescent sensors,[10–12] light emitting diodes,[13] dye sensitized solar cells,[14,15] homo-[16–19] and heterogeneous[20,21] thermo-, electro-,[22] and photocatalysts,[23] and self-healing materials.[24,25] Many of these properties stem from the redox-active couple ($Cu(I) \rightarrow Cu(II) + 1e^-$)[26] and luminescent clusters often designated as secondary building units (SBUs),[9] and a few structure-property relationships have been shown. For instance, the two most encountered SBU motifs are the $Cu_4I_4L_4$ cubane and $Cu_2I_2L_4$ rhomboid (> 80% of occurrence),[6–9] respectively belonging to *globular* and *quasi-planar* motifs. The former category, which includes hexagonal prism[27–29] and fused dicubane,[30–33] is systematically strongly luminescent, whereas the rhomboid motif is mostly either weakly or non-emissive (but not exclusively as rare examples exist).[34] On many occasions, the facile control of the SBU structure, *globular vs. quasi-planar*, mainly cubane $Cu_4I_4L_4$ *vs* rhomboid $Cu_2I_2L_4$, has been performed by simply adjusting the stoichiometric ratio Cu-atom/S-atom, thus controlling the luminescence properties (*on* or *off*).[33,35,36] Generally, the SBU geometry consists of a distinct cluster, but on rare occasions, the SBU motif exhibits a polymeric

1D-$[CuI]_n$ skeleton (**Figure 1**). These 1D-$[CuI]_n$ motifs are accordion ribbon,[37,38] zigzag ribbon,[39] staircase ribbon,[40] and polycubane,[36,41] and again these *quasi-planar* SBUs are either weakly or non-emissive (accordion, zigzag, and staircase ribbons). Concurrently, the *globular* polycubane SBU exhibits an intense emission. The band maxima ($375 < \lambda_{emi} < 540$ nm) and emission lifetimes ($1 < \tau_{emi} < 15$ μs) have been evaluated for a few of these 1D-SBU-containing materials[36–39] and the 1D-polycubane exhibits a the most red-shifted band and longest lifetimes.

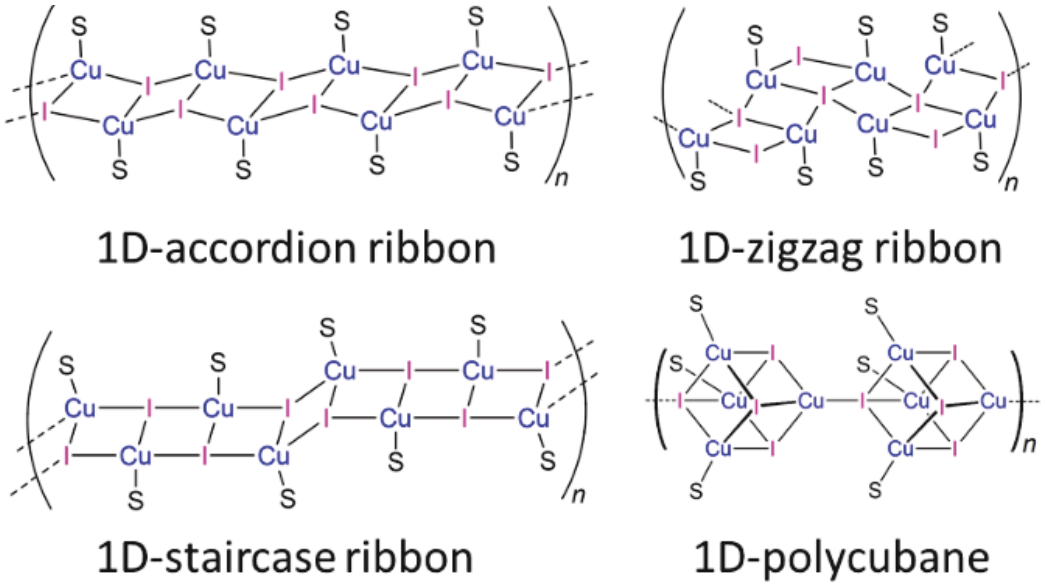

Figure 1. Structures of the 1D-$[CuI]_n$ SBUs encountered in neutral mono- and dithioether / CuI-containing CPs (S = sulfur atom of the thioether ligand).[36–41]

In quest of designing new copper halide/thioether coordination polymers with interesting properties and potential applications[9] and in link with our previous study on $PhS(CH_2)_4SPh$,[29] this work reports two coordination polymers, 1D-$[Cu_4I_4(\mathbf{L1})(MeCN)_2]_n$, **CP1**, and 3D-$[Cu_8I_8(\mathbf{L1})_2]_n$, **CP2** (**L1** = $ArS(CH_2)_4SAr$; Ar = 4-C_6H_4OMe). **CP2** is quite unusual for multiple reasons. First, **CP2** can be prepared in the solid state from **CP1** through a template effect. Second, its SBU exhibits an unprecedented motif, which can be described as a fused poly(truncated rhombic

dodecahedron). Third, the transformation of the emissive **CP1** to the weakly luminescent **CP2** bearing a *globular* SBU drastically differs from what is normally and systematically observed. Fourth, the resulting emission band is in the near-IR region and is now the most red-shifted one and exhibits the shortest lifetimes of all CuX/chalcogenide materials. Fifth, **CP2** exhibits luminescence thermochromism, which is a very rare behaviour for this type of materials. Sixth, **CP2** exhibits a solid-to-solid phase transition at ~100°C with a hysteresis of ~20°C.

RESULTS AND DISCUSSION

The known ligand 1,4-bis(4-methoxyphenyl)thio)butane **L1**[42] was prepared using a modified literature procedure,[43] and its crystal structure (**Figure S1**) and spectroscopic data are placed in the ESI.

*Synthesis of **CP1***. **CP1** is synthesized by reacting CuI with **L1** in a 2:1 mole ratio in acetonitrile (Scheme 1; eq. 1). The mixture is kept at 60°C until the powder is completely dissolved. Upon cooling, transparent crystals suitable for X-ray crystallography started to grow, thus permitting its structure determination (**Figure 2**). No unexpected, new, and/or significant hazards or risks are associated with the reported work.

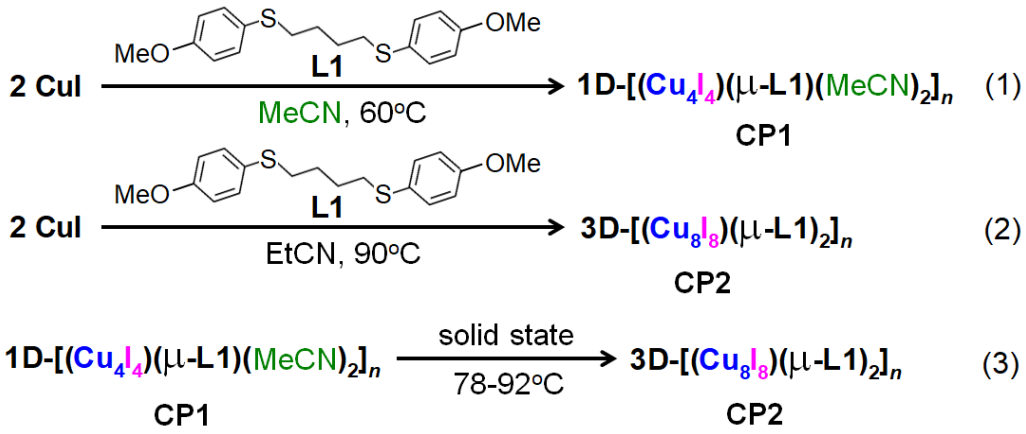

Scheme 1. Syntheses of **CP1** and **CP2**.

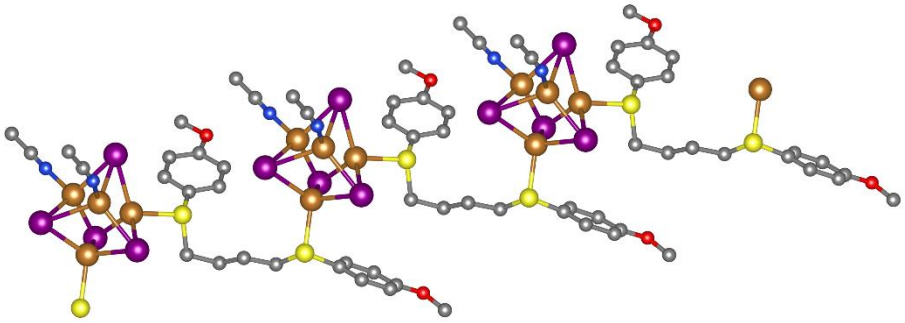

Figure 2. X-ray structure of a segment of **CP1** (brown = Cu, purple = I, yellow = S, red = oxygen, blue = nitrogen, grey = carbon, the H-atoms are not shown for clarity).

The X-ray structure revealed the presence of an alternating 1D [-Cu_4I_4-**L1**-Cu_4I_4-**L1**-]$_n$ chain where the Cu_4I_4 unit exhibits the common closed cubane core, which is ligated by two labile coordinated acetonitrile molecules. Within the dissymmetric Cu_4I_4 cluster, the Cu•••Cu distances range at 100 K from 2.6233(5) to 2.8215(5) Å, the mean bond length of 2.7156(5) Å being inferior to the sum of the van der Waals radii of two Cu atoms (2.8 Å). For comparison, within the 2D network of [Cu_4I_4{μ-PhS$(CH_2)_4$SPh}$_2$]$_n$, a mean bond length of 2.694(15) Å was encountered.[29] There are meanwhile numerous examples of $Cu_4I_4S_4$ clusters (both molecular or as connecting nodes in thioether-based coordination networks) described in the literature, but the structural characterization of a $Cu_4I_4S_2(MeCN)_2$ scaffold bearing two MeCN ligands is hitherto limited to [Cu_4I_4(*N,N'*-bis[2-(cyclohexylthio)ethyl]pyromellitic diimide $(MeCN)_2$]$_n$ and [Cu_4I_4{1,4-bis(2-methylthioethoxy)benzene}$(MeCN)_2$]$_n$.[12,44]

The presence of these nitrile ligands is confirmed by Raman spectroscopy where two ν(C≡N) peaks are observed at 2268 and 2301 cm^{-1} (**Figure S2**), respectively, assigned to the asymmetric and symmetric modes (these signals are too weak to be detected by IR spectroscopy). The elemental analysis is consistent with the formula [Cu_4I_4(**L1**)$(NCMe)_2$] and suggested purity. The

comparison of the powder XRD patterns of a powder sample of **CP1** with the simulated one calculated from its single crystal X-ray data also confirmed homogeneity of the phase except for a medium and a weak intensity scattering at $2\theta = 7.2°$ and 8.9° (red line), which did not match the weak one simulated at 6.9° (black line; **Figure 3**, top).

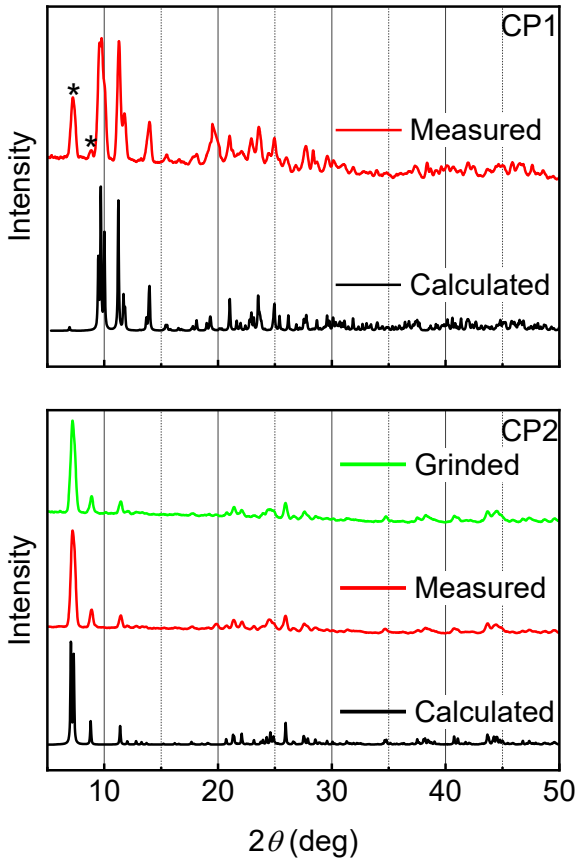

Figure 3. Top: Powder X-ray diffraction patterns calculated (black) and experimental (red) for 1D-$[Cu_4I_4$(**L1**)$(NCMe)_2]_n$ (**CP1**) at 173 K. The calculated and measured diffraction patterns match well with each other, except for two peaks at 7.2° and 8.9° marked with a star. Bottom: Powder X-ray diffraction patterns calculated (black) and experimental on crystals (red) and after grinding (green) for 3D-$[Cu_8I_8$(μ-**L1**)$]_n$ (**CP2**) at 173 K. The calculated and measured diffraction patterns match well with each other, confirming the homogeneity of the crystalline phases.

This finding called for further studies to identify this side species. First, the thermal stability was assessed using TGA (**Figure 4**, left, and **Table 1**). The first weight loss at 96°C corresponds to the loss of about two acetonitrile molecules, then further decomposition occurs at temperature exceeding 200°C. The first weight loss was associated with an endothermic process in the 78-92°C temperature window of the first scan of the DSC traces, which disappeared during the subsequent scans limited to the 55-130°C range (**Figure 5**, left). This transformation from **CP1** into a product having lost these two MeCN molecules is accompanied by recurrent endo- and exothermic processes in the vicinity of 100 and 80°C, respectively, meaning the formation of a new and well-defined species. This process was examined by PXRD (**Figure 5**, right). Upon increasing the temperature, the intensity of the two scatterings at $2\theta = 7.2°$ (plane (0,0,1)) and 8.9° (plane (0,1,1)) increases and becomes dominant, whereas those for **CP1** disappear irreversibly. Upon cooling back to room temperature, the final trace remains intact meaning **CP1** was transformed irreversibly.

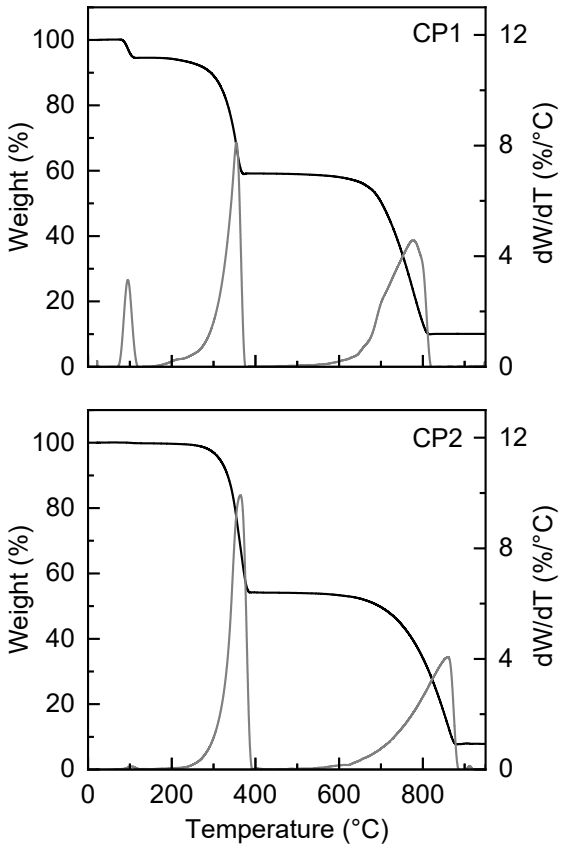

Figure 4. TGA traces (black) and their first derivatives (grey) of **CP1** (top) and **CP2** (bottom) in Ar(g) (25 < T < 950°C).

Table 1. TGA data of **CP1** and **CP2**.

	Formula [M (g.mol^{-1})]	T at dTG_{max} (°C)	$^{Exp}\Delta m$ (%)	$^{Calc}\Delta m$ (%)	**Proposed assignment**
CP1	$C_{22}H_{28}Cu_4I_4N_2O_2S_2$	96	-5.43	-6.97	2MeCN
	[1178.34]	354	-35.42	-33.80	**L**+1/2 I
		776	-49.11	-48.48	$Cu_2I_{3.5}$
CP2	$C_{18}H_{22}Cu_4I_4O_2S_2$	365	-45.81	-45.0	**L**+I+1/2Cu
	[1096.23]	860	-46.37	-46.70	$Cu_2I_{3.5}$

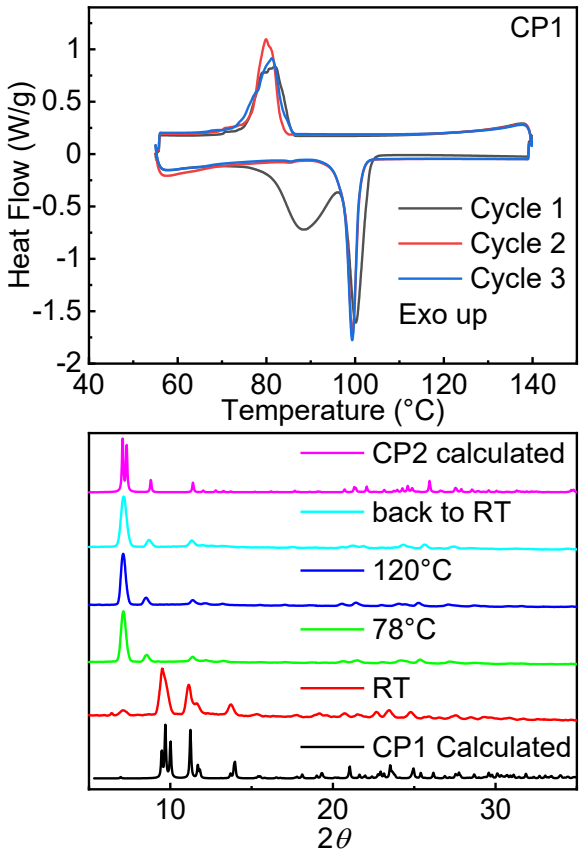

Figure 5. Top: DSC traces of **CP1** under N_2(g). Elimination of MeCN takes placed between 78 and 92°C and leads to the same DSC traces as **CP2**. Bottom: Powder X-ray diffraction patterns for **CP1** calculated (black), at room temperature (red), after heating at 1°C.min^{-1} rate at 78°C (green), 120°C (blue), after cooling back to room temperature (cyan) at 1°C.min^{-1} rate and calculated for **CP2** (pink). Transformation of **CP1** in **CP2** is confirmed by comparing the PXRD of the heated sample *vs.* the calculated profile of **CP2**.

*Synthesis of **CP2***. To identify this air-stable unknown product, this same reaction used to prepare **CP1** was also conducted using EtCN as solvent and kept at 90°C (Scheme 1; eq. 2); a temperature where acetonitrile dissociates from **CP1** (based of both TGA and DSC data). After two hours of heating and allowing to reach ambient temperature, pale yellow X-ray suitable crystals started to grow. Both the Raman and IR spectra indicated absence of any ν(C≡N) peaks

(**Figure S3**). The PXRD (**Figure 5**, bottom) and DSC (**Figure S4**) patterns of **CP2** match well those of the transformation product of **CP1**, thus confirming its identity (Scheme 1; eq. 3).

The X-ray structure reveals formation of a compact 3D-coordination polymer, which may be considered as a non-porous metal-organic framework, of formula $[Cu_8I_8(\mathbf{L1})_2]_n$ (**CP2**) incorporating no coordinated proprionitrile (**Figure 6**). The 3D-construction consists of 2D-diamond-shaped grids built on fused [CuI-SBU-**L1**]$_4$ macrocycles. These SBUs are then fused together to make parallel columnar-$[CuI]_n$ *globular* chains. It is also worth noting that the formation of 3D-networks of $Cu_xX_xL_y$ materials (X = Cl, Br, I; x = 2-8; 4 < y <8) are rare.[6–9] The 4-methoxythiophenyl groups (not shown in **Figure 6**) are filling the cavities inside the macrocycles, which adapt by changing their quasi-planar geometry for a twisted one where both C-S-C bond have rotated. The dimensions of these cavities are defined by the SBU center-to-SBU center within the diamond, which are 12.509, 13.073 and 15.565 Å, **Figure S5**) making this polymer non-porous (analyses, *i.e*. vdW surface, void space %, and void space, using *CrystalMaker*, are provided in **Figure S6**).

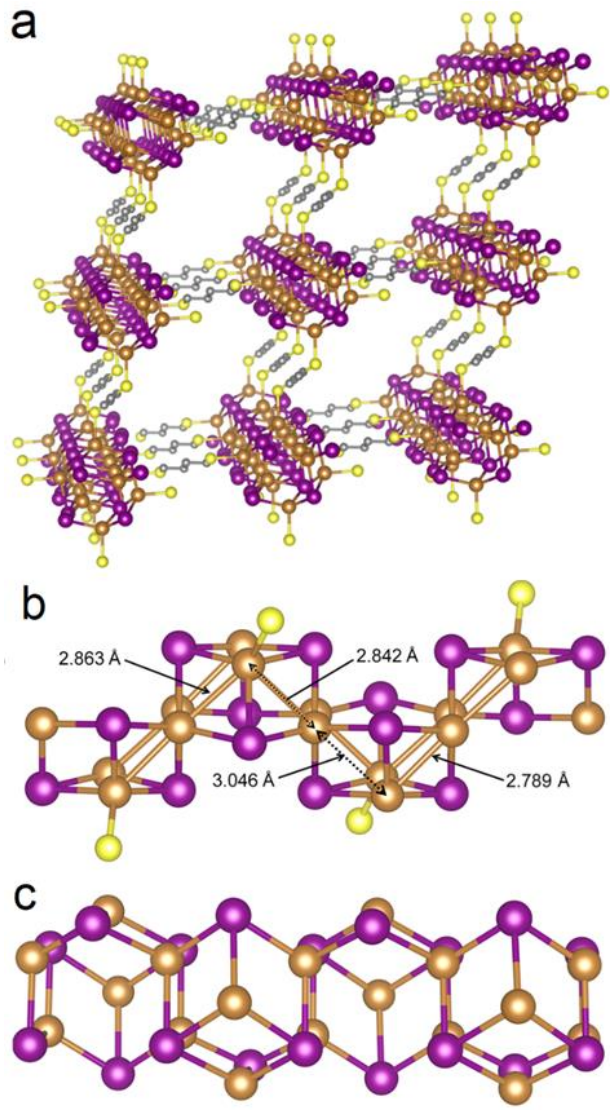

Figure 6. (a) X-ray structure of a segment of the **CP2** (the H-atoms and C_6H_4OMe groups are not shown for clarity; see ESI for all X-ray data; **Tables S2** and **S3**). Purple = I, brown = Cu, yellow = S, grey = carbon. (b, c) Views of the 1D-$[CuI]_n$ motifs with the three shortest Cu•••Cu contacts and the longest (100 K). The remainder of the Cu•••Cu distances are placed in **Table S3**.

More importantly, the 1D-$[CuI]_n$ motif is unprecedented for any CuX chain (X = Cl, Br, I), and consists of a fused 1D-poly(truncated rhombic dodecahedron) (**Figure 7**). Indeed, its structure consists of a 1D-series of centrosymmetric Cu_8I_8 units built upon distorted opened Cu_4I_4 cubanes, where the atoms occupy given positions of a 1D-fused poly(truncated rhombic dodecahedron).

The truncation of the dodecahedron is necessary to secure the alternance between the Cu- and I-atom while keeping the motif neutral. The closest geometry to this 1D-$[CuI]_n$ motif is a fused bi(truncated rhombic dodecahedron) reported as a distinct 0D-$Cu_{10}I_{10}$ SBU found inside a negatively charged coordination polymer $[(Cu_{10}I_{10})(Cu_6I_6)\{(Cu(Bta)_2)_3^-\}]_n$ (Bta = benzotriazole).[45]

In **CP2**, several Cu•••Cu separations approaching the sum of the van der Waals radii (2.80 Å) are observed (**Figure 6**b, **Table S3**) suggesting weak cuprophilic interactions.[46] The variable-temperature measurements of the crystal structure indicate that *(i)* these shortest contacts undergo, counter intuitively, the largest changes with the temperature and that *(ii)* no phase transition occurs between 100 and 300 K (**Figure S6**).

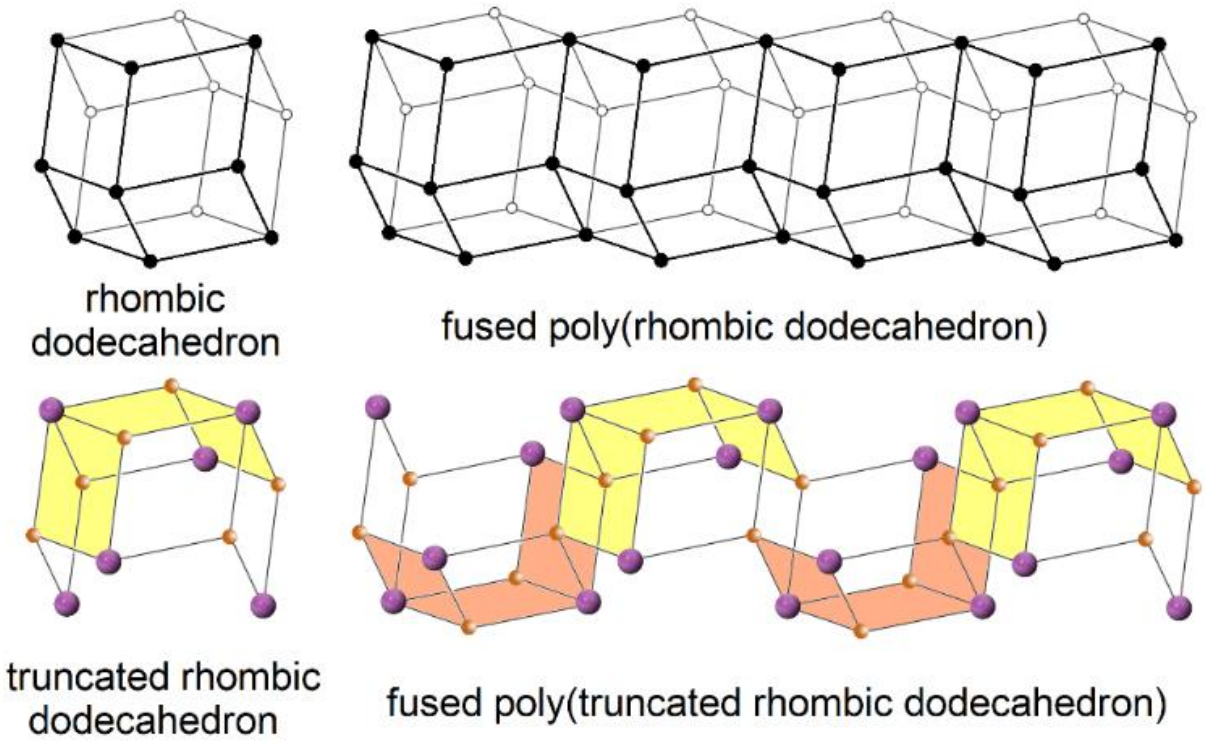

Figure 7. Drawing illustrating the polyhedrons rhombic dodecahedron and truncated rhombic dodecahedron and their corresponding fused 1D-polymers (four units are shown in this segment). The

yellow and brown colours indicate the skeleton origin of the Cu_4I_4 cubanes prior to fusion of the **CP1** chains in the solid state.

Template effect. The structural transformation of a coordination polymer into another upon losing a coordinated ligand and where the SBU changes structure at the same time is rare but not new. An example for such a case was reported by Kim *et al* who reported the solid-state transformation of the non-luminescent 1D-$[Cu_2I_2(\mathbf{L})_2]_n$ into the emissive 2D-$[Cu_4I_4(\mathbf{L})_2]_n$ (**L** = 2-(cyclohexylthio)-1-thiomorpholinoethanone) upon heating.[11] This phase change was accompanied by the loss of a ligand **L** and by the conversion of the rhomboid Cu_2I_2 SBU, which is often weakly or non-emissive emissive, into the luminescent closed cubane Cu_4I_4 SBU. This process was found to be reversible. A similar reversible crystal-to-crystal transformations as a function of temperature and solvent for the $[Cu_4I_4$(*N,N′*-bis[2-(cyclohexylthio)ethyl]pyromellitic diimide $(MeCN)_2]_n$ polymer leading to a luminescence vapochromism phenomenon, was also reported.[12] Quite recently, a rapid and reversible lattice rearrangement triggered by desolvation in a 4,4'-(1,2,4,5-tetrazine-3,6-diyl)dibenzoate-assembled Al(III) MOF has also been observed by several spectroscopic techniques.[47]

Again the SBU in **CP1** is a closed cubane $Cu_4I_4(S)_2(NCMe)_2$ motif (S = thioether), a motif that is well-known.[12,48,49] The generally facile and reversible dissociation of the acetonitrile ligands from closed cubanes without inducing a change in SBU structure conveniently allows for the design of solvent responsive materials.[12,50–52] The absence of rearrangement of the SBUs in the solid state in these literature-documented cases stems from the long distance separating them from one another. Conversely, the transformation of **CP1** into **CP2** is accompanied by a drastic change in SBU structure (cubane → fused poly(truncated rhombic dodecahedron)). This is explained by a predisposed organisation of the $Cu_4I_4(S)_2(NCMe)_2$ units inside the crystal (**Figure**

8). These units are placed in a zigzag fashion and the acetonitrile molecules form a quasi-planar ribbon (**Figure 8**). After thermal extrusion of these acetonitrile molecules, the cubanes exhibit unsaturated sites placed at proximity from each other permitting fusion *via* the formation of Cu-I bonds on both sides, thus leading to the 1D-structure seen in **Figure 6b**. In **Figure 7**, a schematic representation illustrating the origin of the separated Cu_4I_4 cubanes in **CP1** is provided in different colours. In the category of $[Cu_xX_xL_y]$ compounds (X = Cl, Br, I; x = 2-8; 4 < y <8; L = thioether), this template effect is unprecedented.[6–9] Moreover, **CP2** exhibits no evidence for aging even after several months.

The quality of crystals of **CP2** obtained from solution and from solid-state transformation was addressed by comparing their PXRD patterns (Supporting Information). First, the comparison of both patterns is very good as illustrated in Figure 3 for example. The difference between the simulated and experimental exhibits some weak residual comprising both negative and positive components. The degree of similarities (calculated from the software Material Studio) indicates that both crystals are very similar as it is very close (85% (solution) *vs* 80% (solid state)).

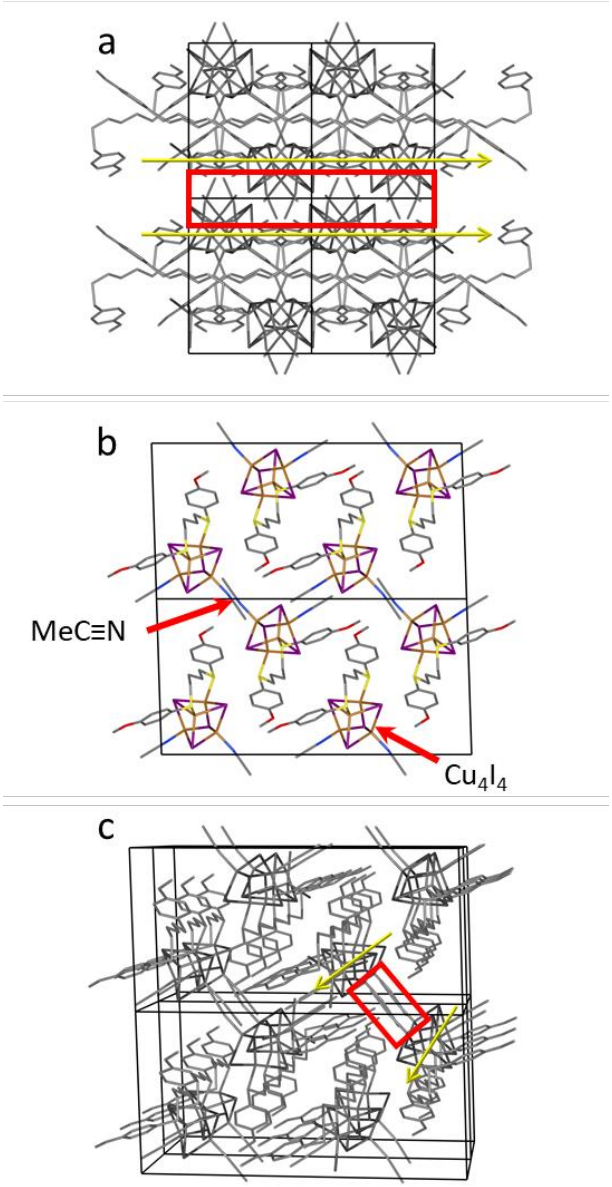

Figure 8. (a) Packing of the 1D-$[Cu_4I_4$(**L1**)$(MeCN)_2]_n$ chains in **CP1** stressing on position of the $Cu_4I_4(S)_2(NCMe)_2$ units belonging to two parallel polymers (see yellow arrows) and the location of the acetonitrile ligands (inside the red rectangle). (b) Another view of the crystal packing stressing on the positions of acetonitrile molecules and cubanes (brown = Cu, purple = I, yellow = S, red = oxygen, blue = nitrogen, grey = carbon, the H-atoms are not shown for clarity). (c) Stereo view of the packing showing the orientation of two parallel chains and position of the labile acetonitrile molecules.

Solid-to-solid phase transition. 3D-CPs and crystalline metal-organic frameworks (MOFs) are not prone to solid-to-solid transitions due to their intrinsic rigidity.[6] Unexpectedly, **CP2** exhibits an unusual thermal behavior associated with a phase transition (**Figure 5** (left), **Figure S4**). The endothermic process appears at ~100°C and the sample remains a solid based on visualisation (**Figure S4**, $T_{transition}$ = 100°C). This thermal process has been confirmed by PXRD and microscopy under white polarized light (**Figure S7**). Upon cooling, the DSC traces exhibit an exothermic crystallization signal in the vicinity of T_{cryst} ~ 80°C. The presence of a hysteresis is interesting, and the temperature gap is ~20°C. For **CP2**, this thermal process may be explained by the sensitive decrease of the crystal density and increase in unit cell volume in function of the temperature (**Figure 9**a,b). At high temperature, sliding motions of the C_6H_4OMe become more facile along with rotation around the C-OMe bonds (**Figure 9**c). In the liquid state, the 1D-$[CuI]_n$ chains gain some degree of freedom along de x (↕) and y axis (↔) (**Figure 9**c,d). The sliding of the aryl groups and rotation around the C-OMe bonds most likely not occur in the same time scale and may explain the presence of the hysteresis.

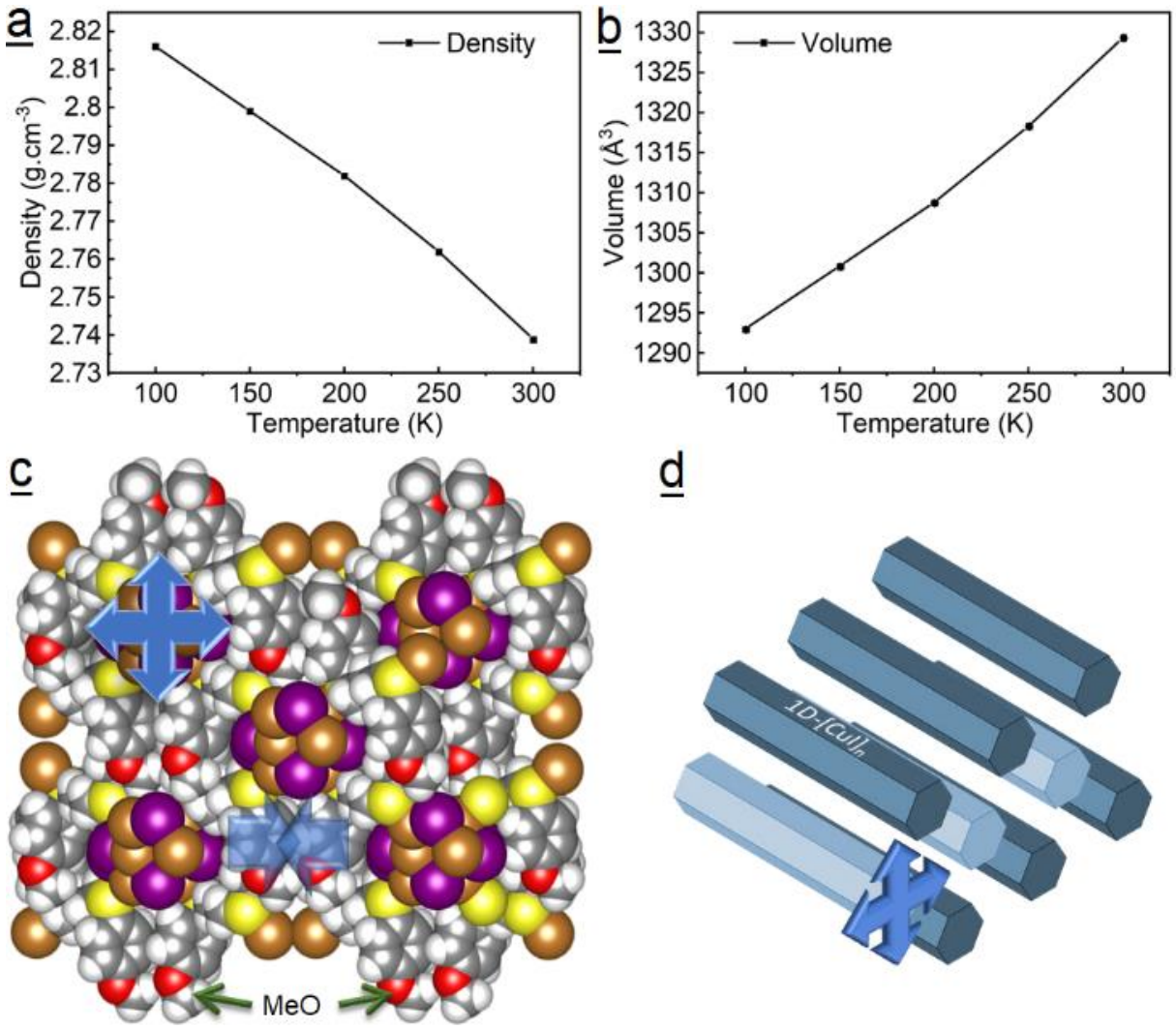

Figure 9. a: Graph reporting density *vs.* temperature for **CP2**. b: Graph reporting volume of the unit cell of **CP2** with the temperature. c: Space filling model of CP2 showing the sliding motions of the C_6H_4OMe groups (transparent arrows) and the degrees of freedom of the 1D-$[CuI]_n$ SBU chains (↕,↔). d: Scheme showing the degrees of freedom (↕,↔) of the 1D-$[CuI]_n$ SBU chains in the liquid state.

*Photophysical properties of **CP1** and **CP2***. Both **CP1** and **CP2** are colorless solids (**Figure S7**) and their absorption bands are in the UV region of the spectra (λ <350 nm; **Figure 10**, black lines). Again, literature proves that $Cu_xI_xS_y$ SBUs exhibiting a *globular* geometry are always

associated with an intense emission.[6–8] In addition, the emission band maxima (λ_{emi}) of cubane-containing species are usually located between ~520 and 620 nm, and exhibit emission lifetimes (τ_{emi}) ranging within the $0.8 < \tau_{emi} < 10$ μs time scale, as either mono- or biphasic decays at 298 K (a recent literature survey of all *globular* shaped SBUs was performed, see SI of ref. 36).[36] Unsurprisingly, this is also the case for **CP1** (**Table 2**). The emission quantum yield ($\Phi_e = 0.35$) compares favorably to that for other *globular* SBUs,[36] and can be seen with naked eyes (**Figure S7**).

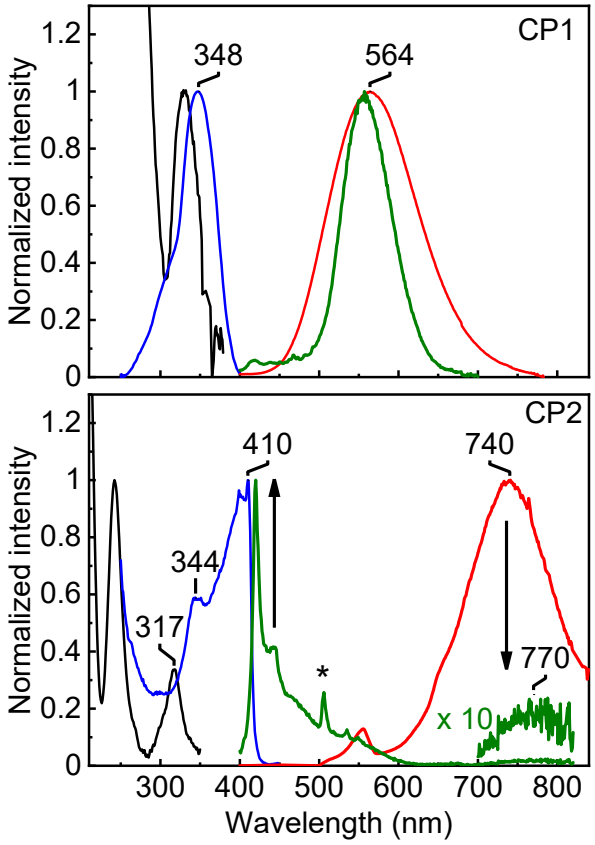

Figure 10. Absorption (black), excitation (blue) and emission (red) spectra of **CP1** (top) and **CP2** (bottom) at 298 K. The green lines are the emission spectra at 77K. It is worth noting that the PXRD patterns match those calculated from the single-crystal X-ray data.

Table 2. Photophysical data of **CP1** and **CP2**.

CP1	**λ_{emi} (nm)**	**τ_{emi} (μs)[a]**	**Φ_e**
298K	564	2.3 (28), 7.2 (72)	0.35
77K	557	2.4 (21), 9.0 (79)	—
CP2	**λ_{emi} (nm)**	**τ_{emi} (ns)[a]**	**Φ_e**
298K	740	0.28 (major), 1.8 (minor)	< 0.0001
77K	770	— [b]	—
77K	420	— [c]	—

[a] The emission decays and curve fitting are placed in **Figures S9** and **S10**.
[b] Too weak to be measured.
[c] Shorter than the excitation pulse (*i.e.* 100 ps).

Conversely, the photophysical behavior of **CP2** significantly differs from **CP1** as the emission extends well in the near-IR (**Figure 10**, bottom). The emission maximum (λ_{max} = 740 nm at 298 K) is placed outside the usual zone (*i.e*. normally expected between ~520 and 620 nm for *globular* SBUs).[36] The large Stoke shift (18000 cm^{-1}) between the absorption (317 nm) and emission (740 nm) bands indicates that the luminescence arises from a triplet excited state. This luminescence cannot be seen with naked eye (**Figure S8**, note that part of the emission band is in the visible region) and the emission quantum yield is smaller than the detection limit of the instrument (Φ_e < 0.0001), which is a notable contrast for a *globular* species. Moreover, the emission lifetimes are in the short ns-time scale, which clearly fall outside the typical μs range. The excessively small Φ_e value is fully consistent with the very short lifetimes. By examining the largest components, the change going from 7.2 μs (**CP1**) to 0.28 ns (**CP2**) represents a decrease of ~26000-fold. By applying this ratio to the quantum yield (0.35 for **CP1**), and assuming that the radiative rate constant, k_e ($k_e = \Phi_e/\tau_{emi}$) is in the same order of magnitude for both coordination polymers, then the expected Φ_e value for **CP2** is ~1 x 10^{-5}, which falls well outside

the sensitivity range of the integration sphere. This ns-time scale for a lower triplet emission lifetime is also consistent with the energy gap law (*i.e.* as the excited state energy decreases, the non-radiative rate constant ($k_{nr} = (1-\Phi_e)/\tau_{emi}$) increases). Moreover, when considering the heavy atom effect, the τ_{emi} values tend to decrease with the number and mass of the nuclei. Altogether, such short lifetimes for low-energy triplet emitters (ns) are unusual but not unprecedented. Indeed, the photophysical properties of the trinuclear cluster $[Pd_3(dppm)_3(CO)](PF_6)_2$ (dppm = $Ph_2PCH_2PPh_2$) was recently reported.[53] In this case, the triplet energy was found at ~8190 cm^{-1} (~1220 nm) and its lifetime (measured from fs-transient absorption spectroscopy) was measured (207 ± 9 ps) at 298 K. Furthermore, a large series of Re(I) complexes was recently investigated and their triplet emission lifetimes were $4.0 < \tau_{emi} < 7.0$ ns at 77 K (other examples are also listed inside reference [54]).

Thermochromism. Thermochromism is an optical phenomenon, notably found in emission. The specific term "luminescence thermochromism" has been coined by Hardt, who investigated this phenomenon during his pioneering work on the $Cu_4I_4(pyridine)_4$ and related clusters.[55]

On some scare occasions, it also has been observed for this category of coordination polymers.[10,56] One investigation pointed out the link between the presence of short Cu•••Cu contacts and thermochromism by virtue of temperature-dependence of this distance.[29] In **CP2**, short distances, close to the sum of the van der Waals radii of two Cu atoms (~2.8 Å), are apparent and are sensitively temperature-dependent (**Table S3**). Upon cooling **CP2** to 77 K, the intensity of the near-IR band decreases drastically (barely observable) and shifts slightly to ~770 nm. Concurrently, a new structured emission band grows at 420 nm, which is an anti-Kasha's emission. This temperature-triggered photoprocess indicates the presence of thermochromism as clearly pointed out in the chromaticity chart (relative positions of the blue and red dots; **Figure**

11). For comparison purposes, the chromatic chart for **CP1** is also presented where no thermochromism is observed (the coordinates at both temperatures are very close to each other).

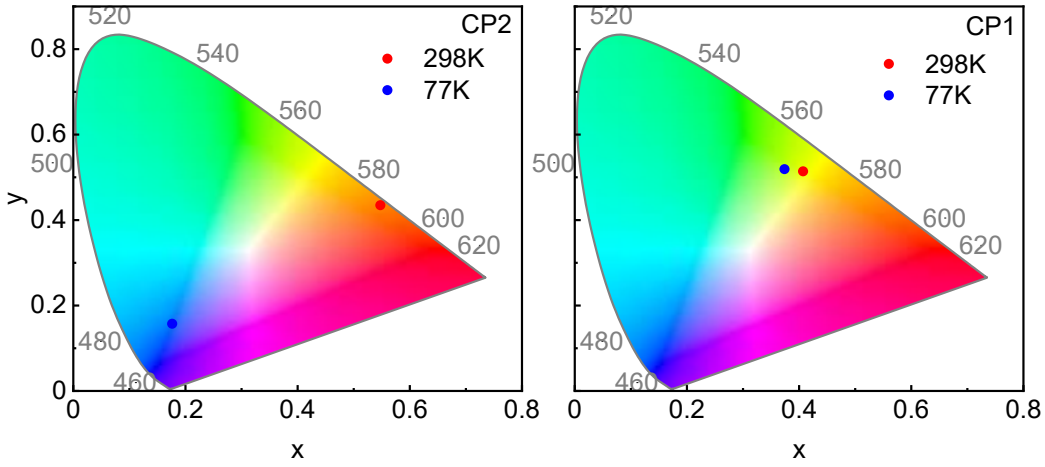

Figure 11. Comparison of the chromaticity charts of **CP1** (left): 298K (0.40713, 0.51402), 77K (0.37385, 0.51913) and **CP2** (right): 298K (0.54754, 0.43484), 77K (0.17631, 0.15737).

The assignment of the 420-nm feature is readily made since it is reminiscent to the phosphorescence band of the free ligand (*i.e.* intraligand ππ*). The solid-state emission of **L1** at 77 K is placed in **Figure S11**. The mirror-image relationship between the excitation (blue trace) and emission signals (green trace; Figure 10 bottom) is also consistent with this assignment. Interestingly, the excitation spectrum exhibiting the ππ* signature was also detected while monitoring the 740-nm band at 298 K. This result indicates that these two excited states, T_n and T_1, are indeed interconnected through internal conversion, the former, T_n, being efficiently populated through intersystem crossing (**Figure 12**). This emission arising from an upper T_n state is reminiscent of that for the classic case of azulene for which the second singlet excited state, S_2, is strongly emissive, whereas S_1 is not.[57] This is again due to the energy gap law. For triplet excited states, this phenomenon has also been observed for platinum(II) containing organometallic conjugated polymers.[58,59] In these cases, the low-lying excited states are charge

transfer ones originating from the conjugated chain (λ_{emi} > 750 nm), whereas the upper triplet excited state, T_n, stems from a localized state of the platinum(II) fragment (λ_{emi} = 450 nm). Moreover, the short-excited state lifetime of this upper T_n emission (< 100 ps) in **CP2** is also consistent with the generally rapid non-radiative depletion of the upper excited states. In conclusion, **CP2** behaves as a temperature-responsive thermochromic material.

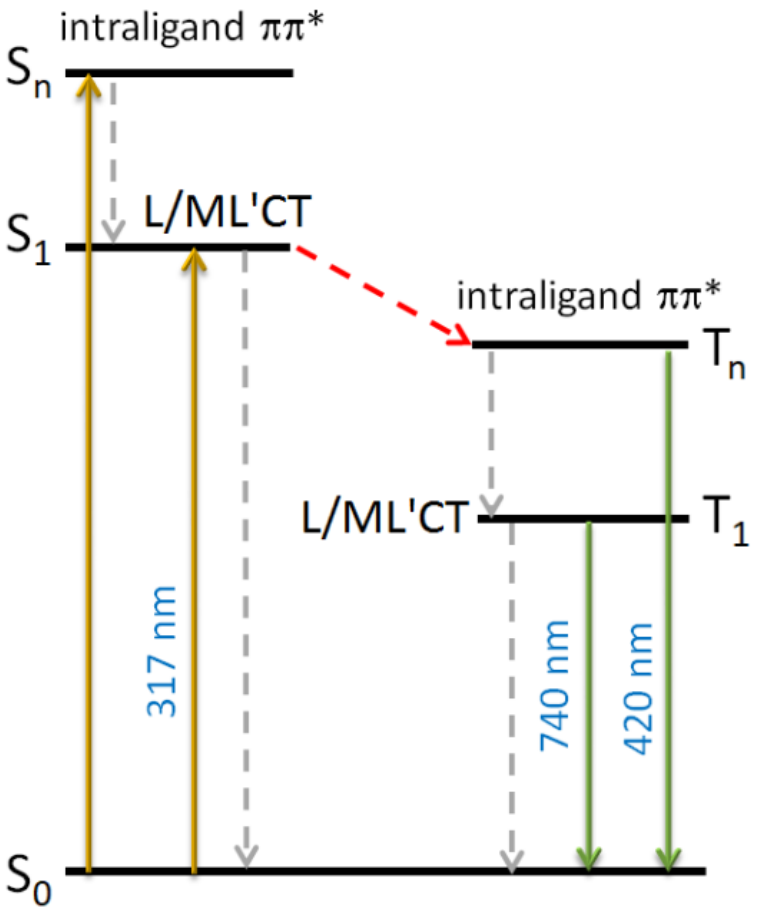

Figure 12. State diagram illustrating the main excited states involved in the photophysical properties of **CP2** (straight lines = radiative processes; dash lines = non-radiative processes, grey = internal conversion, red = intersystem crossing).

The possibility of **CP2** being mechanochromic was also examined. However, both the PXRD patterns and emission band maximum did not change upon grinding the powder in a mortar,

except for a decrease in overall emission intensity (**Figure S12**). The lack of mechanochromism is consistent, and perhaps totally predictable, with the 3D-feature of this coordination polymer, which makes the framework more robust towards mechanical stress.

DFT and TD-DFT computations. All computational data are placed in Figures S13 to S22 and Tables S4 to S9; only selected data are placed in the text. This 1D-$[CuI]_n$ SBU exhibiting an unprecedented motif and unusual photophysical properties called for an assignment for the low-energy singlet and triplet excited states. This important trait was addressed by DFT and TDDFT calculations using two different approaches due to the 1D-nature of this SBU. The first method consists in a periodic computation using the unit cell (DMol3, see detail in the SI) but suffers from a lower degree of accuracy. The second method (Gaussian, B3LYP) is more accurate but cannot be applied to a periodic system due to size limitation. Instead, $[Cu_{14}I_{16}(\mathbf{L1})_8]^{2-}$ was used as model (the use of two extra iodides on each end secures the correct sp^3 hybridization state of all copper atoms). All computational data, for **CP1** and **CP2**, are placed in the SI. **Figure 13** exhibits the frontier MO representations of **CP2** and its model $[Cu_{14}I_{16}(\mathbf{L1})_8]^{2-}$. In both sets of calculations, the HOMO and HOMO-1 exhibit atomic contributions mainly located onto the iodide p-orbitals with minor contributions from the copper metals. In parallel, both sets of calculations for the LUMO+1 and LUMO place the atomic contributions on the π*-system of the phenyl group. Concurrently, the same computations performed on **CP1** lead to the same observations (SI). In conclusion, the nature of the lowest energy singlet excited state is iodide/copper-to-aryl charge transfer (L/ML'CT) in both cases.

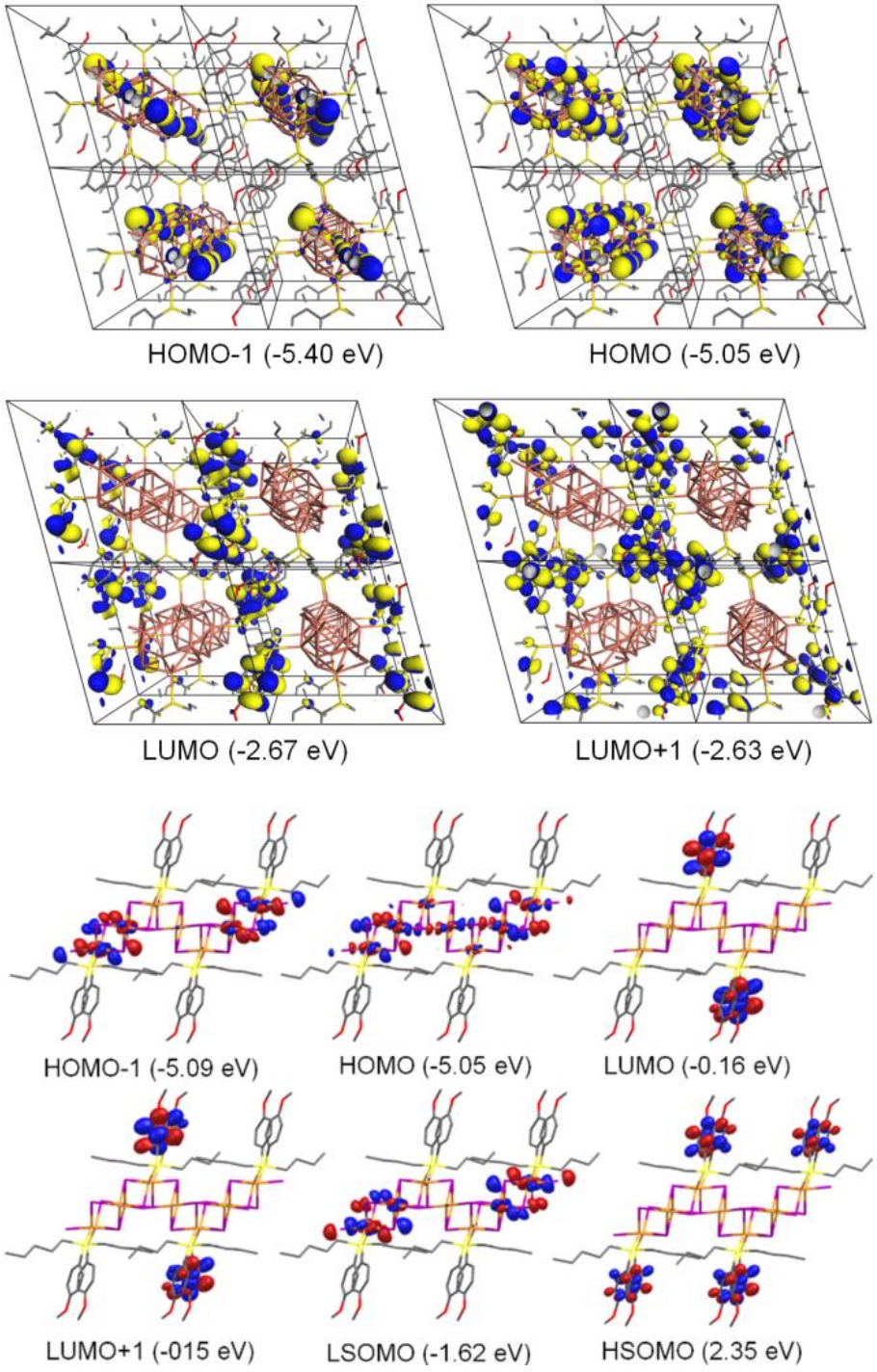

Figure 13. Top: representation of the HOMO-1 ─ LUMO+1 of **CP2** calculated with DMol3. Bottom: Representations of the frontier MOs of the $[Cu_{14}I_{16}(\mathbf{L1})_8]^{2-}$ model in the ground (HOMO-1 ─ LUMO+1) and triplet excited (LSOMO and HSOMO) states. Part of the **L1**'s and H-atoms are omitted for sake of clarity.

Table 3. First 5 calculated spin-allowed electronic transitions of **CP2**.[a]

#	λ (nm)	Osc.St.	Major contributions (%)
1	415.3	0.0015	HOMO→LUMO(98)
2	414.4	0	HOMO→L+1(98)
3	407.1	0.0003	H-1→L+3(22),HOMO→L+3(54),HOMO→L+4(11)
4	406.9	0.0003	H-1→L+5(24),HOMO→L+5(56)
5	402.1	0.0014	HOMO→L+2(90)

[a] See Table S9 for the first 100 spin-allowed electronic transitions.

The TDDFT calculations on the $[Cu_{14}I_{16}(L1)_8]^{2-}$ model (Table 3) indicate that the low-energy transitions are also of the same nature (*i.e*. L/ML'CT). This outcome agrees with that for **CP1** (SI) and that for 2D-$[(Cu_6I_6)(\mu\text{-}PhSCH_2C{\equiv}CCH_2SPh)_3]_n$, for which the SBU is a hexagonal prism.[22] This observation indicates that the nature of the excited states is SBU shape-independent. The low calculated oscillator strengths (F) of the low-energy transitions stem from the poor orbital overlaps between the filled and empty frontier MOs. This computational outcome corroborates the lack of absorptivity in the low energy region of the absorption spectra. Concurrently, the atomic contributions of the low and high semi-occupied MOs (LSOMO and HSOMO; Figure 13 bottom) resemble those of the HOMO-1 and LUMOs, respectively, and indicate that the triplet states are of the same nature ^{3}(M/XLCT)*.

CONCLUSION

Table 4. Specific unique or rare features and properties associated with **CP2**.

	property	comments
1	the SBU is a 1D-$[CuI]_n$ chain	extremely rare according to reviews 6-9
2	fused poly(truncated rhombic dodecahedron) is a unique structure for a SBU	Cambridge crystallographic data bank
3	templated synthesis (from **CP1**)	thus avoiding common decomposition
4	solid-to-solid phase transition	unsuspected for a compact 3D framework
5	most red-shifted emission band	according to reviews 6-9 and refs. herein
6	smallest emission lifetime and quantum yields	according to reviews 6-9 and refs. herein
7	luminescence thermochromism	not rare but very uncommon
8	anti-Kasha's rule	rare

This investigation reported and described a new coordination air stable polymer, **CP2,** which is found to be quite unique as it exhibits several special traits and properties. These features are summarized in Table 4 and commented below. First, its preparation can be performed in both the solid state (from another coordination polymer) or in solution. The solid-state reaction stems from a convenient pre-organized structure (of **CP1**). The macroscopic structure is 3D, which is not common for this category of materials.[6–9] This seemingly compact and robust 3D-scaffolding is consistent with the absence of mechanochromism and the fact that no evidence for aging was observed for several months, and yet an unexpected solid-to-solid phase transition is depicted. The SBU falls in the rare category of 1D-polymeric SBUs 1-$[CuX]_n$ (X = Cl, Br, I, CN, SCN).[6–9] In fact, the poly(truncated rhomboid dodecahedron) structure has never been observed before throughout the literature according to a Cambridge Crystallographic Data Centre survey. This original SBU belongs to the *globular* category, which normally is intensively emissive with band maxima ranging from ~520 to 620 nm at room temperature with emission decaying in the μs

time scale, but all resulting photophysical features fall well outside these properties. Indeed, with an emission maximum at ~740 nm, this material is considered a near-IR phosphor. In addition, it exhibits thermochromism as unambiguously demonstrated by the chromaticity charts. This property is driven by a sensitive decrease of the Cu•••Cu distances upon cooling (witnessed by a red shift of the emission band) also resulting into a decrease in its intensity (energy gap law). The dominant emission at low temperature then becomes one arising from an upper intraligand triplet excited state, which makes then this material not following the Kasha's rule. Finally, it is noteworthy that **CP2** can be straightforwardly prepared in a gram scale and can resist aging processes even upon exposure to air after several months.

A recent review pointed out that this category of materials (*i.e.* copper halide/chalcogenide coordination polymers) exhibits a large brochette of interesting properties and applications.[9] All in all, these (quite numerous) unusual traits resulting from the conversion of one coordination polymer into another simply upon a gentle thermal elimination of the labile acetonitrile ligands. Literature reports countless X-ray structures of coordination materials exhibiting labile ligands linked to various 0D, 1D, and 2D-species. Without further treatments of these meta-stable and reactive intermediates, the observations made in this current study strongly suggests that quite many of these literature investigations may have missed the opportunity to discover new materials exhibiting new properties and applications.

ASSOCIATED CONTENT

Supporting Information. Experimental procedure for synthesis of ligands and CPs, instrumentation and computational details, summary of X-ray data collection, IR and Raman

spectra, DSC curves, polarized light microscopy images, absorption, emission and excitation and lifetimes at 298 and 77 K of emissive species, computational results.

Accession Codes. CCDC 2048036, 2048037, 2048041, 2048042, 2048044, 2048045 and 2048050 contain the supplementary crystallographic data for this paper. These data can be obtained free of charge via www.ccdc.cam.ac.uk/data_request/cif,orby emailing data_request@ccdc.cam.ac.uk, or by contacting The Cambridge Crystallographic Data Centre, 12 Union Road, Cambridge CB2 1EZ, UK; fax: +44 1223 336033.

AUTHOR INFORMATION

Corresponding Author

*E-mail: Pierre.Harvey@USherbrooke.ca (P.D.H.)

*E-mail: Michael.Knorr@univ-fcomte.fr (M.K.).

Author Contributions

Conceptualization, M.K. and P.D.H.; methodology, A.S.; software, K.T.; validation, A.S., M.K. and P.D.H.; formal analysis, A.S.; investigation, A.S., K.T., R.S. and P.L.K; resources, P.D.H., M.K. and C.S.; data curation, A.S.; writing—original draft preparation, P.D.H. ; writing—review and editing, A.S., M.K. and P.D.H.; visualization, A.S.; supervision, P.D.H., M.K. and C.S.; project administration, A.S.; funding acquisition, P.D.H. and M.K.. All authors have read and agreed to the published version of the manuscript.

Notes

The authors declare no competing financial interest.

ACKNOWLEDGMENT

This work was supported by the Natural Sciences and Engineering Research Council of Canada, the Fonds de Recherche du Québec-Nature et Technologies, Compute Canada and Calcul Québec and the Centre Quebecois sur les Matériaux Fonctionnels. Miss J. Plé (Ms.C.) is thanked for some preliminary investigations. M.K. and C.S. thank the CNRS and the DFG for financial support.

REFERENCES

(1) Ford, P. C.; Cariati, E.; Bourassa, J. Photoluminescence Properties of Multinuclear Copper(I) Compounds. *Chem. Rev.* **1999**, *99* (12), 3625–3647. https://doi.org/10.1021/cr960109i.

(2) Conesa-Egea, J.; Zamora, F.; Amo-Ochoa, P. Perspectives of the Smart Cu-Iodine Coordination Polymers: A Portage to the World of New Nanomaterials and Composites. *Coord. Chem. Rev.* **2019**, *381*, 65–78. https://doi.org/10.1016/j.ccr.2018.11.008.

(3) Liu, W.; Fang, Y.; Li, J. Copper Iodide Based Hybrid Phosphors for Energy-Efficient General Lighting Technologies. *Adv. Funct. Mater.* **2018**, *28* (8), 1705593. https://doi.org/10.1002/adfm.201705593.

(4) Kobayashi, A.; Kato, M. Stimuli-Responsive Luminescent Copper(I) Complexes for Intelligent Emissive Devices. *Chem. Lett.* **2017**, *46* (2), 154–162. https://doi.org/10.1246/cl.160794.

(5) Ardizzoia, G. A.; Brenna, S. Hydroxo-Bridged Copper(II) Cubane Complexes. *Coord. Chem. Rev.* **2016**, *311*, 53–74. https://doi.org/10.1016/j.ccr.2015.11.013.

(6) Harvey, P. D.; Knorr, M. Designs of 3-Dimensional Networks and MOFs Using Mono- and Polymetallic Copper(I) Secondary Building Units and Mono- and Polythioethers: Materials Based on the Cu–S Coordination Bond. *J. Inorg. Organomet. Polym. Mater.* **2016**, *26* (6), 1174–1197.

https://doi.org/10.1007/s10904-016-0378-7.

(7) Harvey, P. D.; Knorr, M. Stabilization of (CuX)n Clusters (X = Cl, Br, I; n = 2, 4, 5, 6, 8) in Mono- and Dithioether-Containing Layered Coordination Polymers. *J. Clust. Sci.* **2015**, *26* (2), 411–459. https://doi.org/10.1007/s10876-014-0831-0.

(8) Harvey, P. D.; Knorr, M. Luminescent Coordination Polymers Built upon Cu4X4 (X=Br,I) Clusters and Mono- and Dithioethers. *Macromol. Rapid Commun.* **2010**, *31* (9–10), 808–826. https://doi.org/10.1002/marc.200900893.

(9) Schlachter, A.; Harvey, P. D. Properties and Applications of Copper Halide-Chalcogenoether and -Chalcogenone Networks and Functional Materials. *J. Mater. Chem. C* **2021**, *9* (21), 6648–6685. https://doi.org/10.1039/d1tc00585e.

(10) Kim, T. H.; Shin, Y. W.; Jung, J. H.; Kim, J. S.; Kim, J. Crystal-to-Crystal Transformation between Three CuI Coordination Polymers and Structural Evidence for Luminescence Thermochromism. *Angew. Chem. Int. Ed.* **2008**, *47* (4), 685–688. https://doi.org/10.1002/anie.200704349.

(11) Jai, Y. L.; So, Y. L.; Sim, W.; Park, K. M.; Kim, J.; Shim, S. L. Temperature-Dependent 3-D CuI Coordination Polymers of Calix[4]-Bis- Dithiacrown: Crystal-to-Crystal Transformation and Photoluminescence Change on Coordinated Solvent Removal. *J. Am. Chem. Soc.* **2008**, *130* (22), 6902–6903. https://doi.org/10.1021/ja8008693.

(12) Kang, G.; Jeon, Y.; Lee, K. Y.; Kim, J.; Kim, T. H. Reversible Luminescence Vapochromism and Crystal-to-Amorphous-to-Crystal Transformations of Pseudopolymorphic Cu(I) Coordination Polymers. *Cryst. Growth Des.* **2015**, *15* (11), 5183–5187. https://doi.org/10.1021/acs.cgd.5b01199.

(13) He, J.; Huang, J.; He, Y.; Cao, P.; Zeller, M.; Hunter, A. D.; Xu, Z. A Boiling-Water-Stable,

Tunable White-Emitting Metal-Organic Framework from Soft-Imprint Synthesis. *Chem. Eur. J.* **2016**, *22* (5), 1597–1601. https://doi.org/10.1002/chem.201504941.

(14) Tanaka, N.; Okubo, T.; Anma, H.; Kim, K. H.; Inuzuka, Y.; Maekawa, M.; Kuroda-Sowa, T. Halido-Bridged 1D Mixed-Valence CuI-CuII Coordination Polymers Bearing a Piperidine-1-Carbodithioato Ligand: Crystal Structure, Magnetic and Conductive Properties, and Application in Dye-Sensitized Solar Cells. *Eur. J. Inorg. Chem.* **2013**, *2013* (19), 3384–3391. https://doi.org/10.1002/ejic.201300188.

(15) Okubo, T.; Tanaka, N.; Anma, H.; Kim, K. H.; Maekawa, M.; Kuroda-Sowa, T. Dye-Sensitized Solar Cells with New One-Dimensional Halide-Bridged Cu(I)-Ni(II) Heterometal Coordination Polymers Containing Hexamethylene Dithiocarbamate Ligand. *Polymers* **2012**, *4* (3), 1613–1626. https://doi.org/10.3390/polym4031613.

(16) Akhmetova, V. R.; Akhmadiev, N. S.; Nurtdinova, G. M.; Yanybin, V. M.; Glazyrin, A. B.; Ibragimov, A. G. S,S-Complexes of Copper(I) Halides with 1,2-Bis(3,5-Dimethyloxazol-4-Ylmethylsulfanyl)Ethane as New Catalysts for Phenylacetylene Aminomethylation. *Russ. J. Gen. Chem.* **2018**, *88* (7), 1418–1424. https://doi.org/10.1134/S1070363218070113.

(17) Saha, S.; Biswas, K.; Basu, B. 1-D Copper(I) Coordination Polymer Based on Bidentate 1,3-Dithioether Ligand: Novel Catalyst for Azide-Alkyne-Cycloaddition (AAC) Reaction. *Tetrahedron Lett.* **2018**, *59* (26), 2541–2545. https://doi.org/10.1016/j.tetlet.2018.05.040.

(18) Saha, S.; Biswas, K.; Ghosh, P.; Basu, B. New 1,2-Dithioether Based 2D Copper(I) Coordination Polymer: From Synthesis to Catalytic Application in A3-Coupling Reaction. *J. Coord. Chem.* **2019**, *72* (11), 1810–1819. https://doi.org/10.1080/00958972.2019.1627339.

(19) Ji, W.; Qu, J.; Jing, S.; Zhu, D.; Huang, W. Copper(i) Halide Clusters Based upon Ferrocenylchalcogenoether Ligands: Donors, Halides and Semi-Rigidity Effects on the Geometry

and Catalytic Activity. *Dalton Trans.* **2016**, *45* (3), 1016–1024. https://doi.org/10.1039/c5dt03993b.

(20) Gahlot, S.; Jeanneau, E.; Dappozze, F.; Guillard, C.; Mishra, S. Precursor-Mediated Synthesis of Cu2-XSe Nanoparticles and Their Composites with TiO2 for Improved Photocatalysis. *Dalton Trans.* **2018**, *47* (27), 8897–8905. https://doi.org/10.1039/c8dt01625a.

(21) Ji, W.; Qu, J.; Li, C. A.; Wu, J. W.; Jing, S.; Gao, F.; Lv, Y. N.; Liu, C.; Zhu, D. R.; Ren, X. M.; Huang, W. In Situ Surface Assembly of Core-Shell TiO2-Copper(I) Cluster Nanocomposites for Visible-Light Photocatalytic Reduction of Cr(VI). *Appl. Catal. B Environ.* **2017**, *205*, 368–375. https://doi.org/10.1016/j.apcatb.2016.12.041.

(22) Li, C. A.; Ji, W.; Qu, J.; Jing, S.; Gao, F.; Zhu, D. R. A PEG/Copper(i) Halide Cluster as an Eco-Friendly Catalytic System for C-N Bond Formation. *Dalton Trans.* **2018**, *47* (22), 7463–7470. https://doi.org/10.1039/c8dt01310a.

(23) Ji, W.; Wang, H.; Li, C. A.; Gao, F.; An, Z. F.; Huang, L.; Wang, H.; Pan, Y.; Zhu, D. R.; Wang, J. Q.; Guo, C.; Mayoral, J. A.; Jing, S. Cuprous Cluster as Effective Single-Molecule Metallaphotocatalyst in White Light-Driven C[Sbnd]H Arylation. *J. Catal.* **2019**, *378*, 270–276. https://doi.org/10.1016/j.jcat.2019.08.017.

(24) Zhang, J.; Li, M.; Cheng, L.; Li, T. Multifunctional Polymers Built on Copper-Thioether Coordination. *Polym. Chem.* **2017**, *8* (42), 6527–6533. https://doi.org/10.1039/c7py01359k.

(25) Liu, Y.; Peng, H.; Wu, P.; Liu, H.; Zhang, J. Stretchable and Luminescent Networks from Copper(I)-Coordinated Main-Chain Thioether Polymers. *Polymer (Guildf).* **2019**, *179*, 121616. https://doi.org/10.1016/j.polymer.2019.121616.

(26) Rasouli, M.; Morshedi, M.; Amirnasr, M.; Z. Slawin, A. M.; Randall, R. Synthesis, Crystal Structure, and Electrochemical Properties of Cu(I) Coordination Polymers with Two New (NS) 2

Schiff-Base Ligands Containing Long Flexible Spacers . *J. Coord. Chem.* **2013**, *66* (11), 1974–1984. https://doi.org/10.1080/00958972.2013.796370.

(27) Bai, S. Q.; Wong, I. H. K.; Zhang, N.; Lin Ke, K.; Lin, M.; Young, D. J.; Hor, T. S. A. A New 3-D Coordination Polymer as a Precursor for CuI-Based Thermoelectric Composites. *Dalton Trans.* **2018**, *47* (45), 16292–16298. https://doi.org/10.1039/c8dt03219j.

(28) Aly, S. M.; Pam, A.; Khatyr, A.; Knorr, M.; Rousselin, Y.; Kubicki, M. M.; Bauer, J. O.; Strohmann, C.; Harvey, P. D. Cluster-Containing Coordination Polymers Built Upon (Cu2I2S2)m Units (m = 2, 3) and ArSCH2C≡CCH2SAr Ligands: Is the Cluster Size Dependent Upon Steric Hindrance or Ligand Rigidity? *J. Inorg. Organomet. Polym. Mater.* **2014**, *24* (1), 190–200. https://doi.org/10.1007/s10904-013-9984-9.

(29) Knorr, M.; Guyon, F.; Khatyr, A.; Däschlein, C.; Strohmann, C.; Aly, S. M.; Abd-El-Aziz, A. S.; Fortin, D.; Harvey, P. D. Rigidity effect of the dithioether spacer on the size of the luminescent cluster (Cu2I2)n (n = 2, 3) in their coordination polymers. *Dalton Trans.* **2009**, *0* (6), 948–955. https://doi.org/10.1039/b816987j.

(30) Bonnot, A.; Juvenal, F.; Lapprand, A.; Fortin, D.; Knorr, M.; Harvey, P. D. Can a Highly Flexible Copper(i) Cluster-Containing 1D and 2D Coordination Polymers Exhibit MOF-like Properties? *Dalton Trans.* **2016**, *45* (28), 11413–11421. https://doi.org/10.1039/c6dt01375a.

(31) Knorr, M.; Bonnot, A.; Lapprand, A.; Khatyr, A.; Strohmann, C.; Kubicki, M. M.; Rousselin, Y.; Harvey, P. D. Reactivity of CuI and CuBr toward Dialkyl Sulfides RSR: From Discrete Molecular Cu4I4S4 and Cu8I8S6 Clusters to Luminescent Copper(I) Coordination Polymers. *Inorg. Chem.* **2015**, *54* (8), 4076–4093. https://doi.org/10.1021/acs.inorgchem.5b00327.

(32) Harvey, P. D.; Bonnot, A.; Lapprand, A.; Strohmann, C.; Knorr, M. Coordination RC6H4S(CH2)8SC6H4R/(CuI)n Polymers (R (n) = H (4); Me (8)): An Innocent Methyl Group

That Makes the Difference. *Macromol. Rapid Commun.* **2015**, *36* (7), 654–659. https://doi.org/10.1002/marc.201400659.

(33) Schlachter, A.; Viau, L.; Fortin, D.; Knauer, L.; Strohmann, C.; Knorr, M.; Harvey, P. D. Control of Structures and Emission Properties of (CuI)n 2-Methyldithiane Coordination Polymers. *Inorg. Chem.* **2018**, *57* (21), 13564–13576. https://doi.org/10.1021/acs.inorgchem.8b02168.

(34) Knorr, M.; Guyon, F.; Khatyr, A.; Allain, M.; Aly, S. M.; Lapprand, A.; Fortin, D.; Harvey, P. D. Unexpected Formation of a Doubly Bridged Cyclo-1,2-Dithian 1D Coordination Cu 2I 2-Containing Luminescent Polymer. *J. Inorg. Organomet. Polym. Mater.* **2010**, *20* (3), 534–543. https://doi.org/10.1007/s10904-010-9389-y.

(35) Knorr, M.; Guyon, F.; Khatyr, A.; Strohmann, C.; Allain, M.; Aly, S. M.; Lapprand, A.; Fortin, D.; Harvey, P. D. Construction of (CuX) 2n Cluster-Containing (X = Br, I; N = 1, 2) Coordination Polymers Assembled by Dithioethers ArS(CH 2) MSAr (Ar = Ph, p-Tol; M = 3, 5): Effect of the Spacer Length, Aryl Group, and Metal-to-Ligand Ratio on the Dimensionality, Cluster . *Inorg. Chem.* **2012**, *51* (18), 9917–9934. https://doi.org/10.1021/ic301385u.

(36) Schlachter, A.; Lapprand, A.; Fortin, D.; Strohmann, C.; Harvey, P. D.; Knorr, M. From Short-Bite Ligand Assembled Ribbons to Nanosized Networks in Cu(I) Coordination Polymers Built Upon Bis(Benzylthio)Alkanes (BzS(CH 2) n SBz; n = 1–9). *Inorg. Chem.* **2020**, *59* (6), 3686–3708. https://doi.org/10.1021/acs.inorgchem.9b03275.

(37) Bonnot, A.; Knorr, M.; Guyon, F.; Kubicki, M. M.; Rousselin, Y.; Strohmann, C.; Fortin, D.; Harvey, P. D. 1,4-Bis(Arylthio)but-2-Enes as Assembling Ligands for (Cu2X2)n (X = I, Br; N = 1, 2) Coordination Polymers: Aryl Substitution, Olefin Configuration, and Halide Effects on the Dimensionality, Cluster Size, and Luminescence Properties. *Cryst. Growth Des.* **2016**, *16* (2), 774–788. https://doi.org/10.1021/acs.cgd.5b01360.

(38) Raghuvanshi, A.; Knorr, M.; Knauer, L.; Strohmann, C.; Boullanger, S.; Moutarlier, V.; Viau, L. 1,3-Dithianes as Assembling Ligands for the Construction of Copper(I) Coordination Polymers. Investigation of the Impact of the RC(H)S 2 C 3 H 6 Substituent and Reaction Conditions on the Architecture of the 0D-3D Networks. *Inorg. Chem.* **2019**, *58* (9), 5753–5775. https://doi.org/10.1021/acs.inorgchem.9b00114.

(39) Raghuvanshi, A.; Dargallay, N. J.; Knorr, M.; Viau, L.; Knauer, L.; Strohmann, C. 1,3-Dithiolane and 1,3-Ferrocenyl-Dithiolane as Assembling Ligands for the Construction of Cu(I) Clusters and Coordination Polymers. *J. Inorg. Organomet. Polym. Mater.* **2017**, *27* (5), 1501–1513. https://doi.org/10.1007/s10904-017-0610-0.

(40) Knorr, M.; Guyon, F. Luminescent Oligomeric and Polymeric Copper Coordination Compounds Assembled by Thioether Ligands. In *Macromolecules Containing Metal and Metal-Like Elements*; Abd-El Aziz, A. S., Carraher, C. E., Harvey, P. D., Pittman, C. U., Zeldin, M., Eds.; John Wiley & Sons, Inc.: Hoboken, NJ, USA, 2010; Vol. 10, pp 89–158. https://doi.org/10.1002/9780470604090.ch3.

(41) Xie, C.; Zhou, L.; Feng, W.; Wang, J.; Chen, W. Varying the Frameworks of Coordination Polymers with (CuI)4 Cubane Cluster by Altering Terminal Groups of Thioether Ligands. *J. Mol. Struct.* **2009**, *921* (1–3), 132–136. https://doi.org/10.1016/j.molstruc.2008.12.043.

(42) Baliah, V.; Aparajithan, K. Dipole Moments and UV Spectra of Some Long-Chain Molecules. *J. Indian Chem. Soc.* **1992**, *69* (5), 255–259.

(43) Hartley, F. R.; Murray, S. G.; Levason, W.; Soutter, H. E.; McAuliffe, C. A. Systematics of Palladium(II) and Platinum(II) Dithioether Complexes. The Effect of Ligand Structure upon the Structure and Spectra of the Complexes and upon Inversion at Coordinated Sulphur. *Inorganica Chim. Acta* **1979**, *35* (C), 265–277. https://doi.org/10.1016/S0020-1693(00)93450-9.

(44) Kim, T. H.; Yang, H.; Park, G.; Lee, K. Y.; Kim, J. Γ-Cui Nanocrystals From Self-Assembled Coordination Polymers. *Chem. - An Asian J.* **2010**, *5* (2), 252–255. https://doi.org/10.1002/asia.200900416.

(45) Wu, T.; Li, M.; Li, D.; Huang, X. C. Anionic Cu Ni n Cluster-Based Architectures Induced by in Situ Generated N-Alkylated Cationic Triazolium Salts. *Cryst. Growth Des.* **2008**, *8* (2), 568–574. https://doi.org/10.1021/cg070639f.

(46) Harisomayajula, N. V. S.; Makovetskyi, S.; Tsai, Y. C. Cuprophilic Interactions in and between Molecular Entities. *Chem. Eur. J.* **2019**, *25* (38), 8936–8954. https://doi.org/10.1002/chem.201900332.

(47) Lo, S.-H.; Feng, L.; Tan, K.; Huang, Z.; Yuan, S.; Wang, K.-Y.; Li, B.-H.; Liu, W.-L.; Day, G. S.; Tao, S.; Yang, C.-C.; Luo, T.-T.; Lin, C.-H.; Wang, S.-L.; Billinge, S. J. L.; Lu, K.-L.; Chabal, Y. J.; Zou, X.; Zhou, H.-C. Rapid Desolvation-Triggered Domino Lattice Rearrangement in a Metal–Organic Framework. *Nat. Chem.* **2020**, *12* (1), 90–97. https://doi.org/10.1038/s41557-019-0364-0.

(48) Martínez-Alanis, P. R.; Ugalde-Saldívar, V. M.; Castillo, I. Electrochemical and Structural Characterization of Tri- and Dithioether Copper Complexes. *Eur. J. Inorg. Chem.* **2011**, *2011* (2), 212–220. https://doi.org/10.1002/ejic.201000960.

(49) Knorr, M.; Khatyr, A.; Dini Aleo, A.; El Yaagoubi, A.; Strohmann, C.; Kubicki, M. M.; Rousselin, Y.; Aly, S. M.; Fortin, D.; Lapprand, A.; Harvey, P. D. Copper(I) Halides (X = Br, I) Coordinated to Bis(Arylthio)Methane Ligands: Aryl Substitution and Halide Effects on the Dimensionality, Cluster Size, and Luminescence Properties of the Coordination Polymers. *Cryst. Growth Des.* **2014**, *14* (11), 5373–5387. https://doi.org/10.1021/cg500905z.

(50) Kim, S.; Siewe, A. D.; Lee, E.; Ju, H.; Park, I. H.; Park, K. M.; Ikeda, M.; Habata, Y.; Lee, S. S. Ligand-Induced Formation of Copper(I) Iodide Clusters: Exocyclic Coordination Polymers with

Bis-Dithiamacrocycle Isomers. *Inorg. Chem.* **2016**, *55* (5), 2018–2022. https://doi.org/10.1021/acs.inorgchem.5b02314.

(51) Jai, Y. L.; Hyun, J. K.; Jong, H. J.; Sim, W.; Shim, S. L. Networking of Calixcrowns: From Heteronuclear Endo/Exocyclic Coordination Polymers to A Photoluminescence Switch. *J. Am. Chem. Soc.* **2008**, *130* (42), 13838–13839. https://doi.org/10.1021/ja805337n.

(52) Kim, T. H.; Lee, S.; Jeon, Y.; Shin, Y. W.; Kim, J. Reversible Photoluminescence Switch: A Stair-Step Cu4I 4 Coordination Polymer Based on a Dithioether Ligand. *Inorg. Chem. Commun.* **2013**, *33*, 114–117. https://doi.org/10.1016/j.inoche.2013.04.018.

(53) Luo, P.; Karsenti, P. L.; Marsan, B.; Harvey, P. D. Triplet Energy Transfers in Well-Defined Host-Guest Porphyrin-Carboxylate/Cluster Assemblies. *Inorg. Chem.* **2016**, *55* (9), 4410–4420. https://doi.org/10.1021/acs.inorgchem.6b00185.

(54) Schlachter, A.; Juvenal, F.; Kinghat Tangou, R.; Khatyr, A.; Guyon, F.; Karsenti, P.-L.; Strohmann, C.; Kubicki, M. M.; Rousselin, Y.; Harvey, P. D.; Knorr, M. 2-Azabutadiene Complexes of Rhenium(i): S , N -Chelated Species with Photophysical Properties Heavily Governed by the Ligand Hidden Traits. *Dalton Trans.* **2021**, *50* (8), 2945–2963. https://doi.org/10.1039/d0dt04183a.

(55) Hardt, H. D.; Pierre, A. Fluorescence Thermochromism and Symmetry of Copper(I) Complexes. *Inorganica Chim. Acta* **1977**, *25* (C), L59–L60. https://doi.org/10.1016/S0020-1693(00)95644-5.

(56) Horike, S.; Nagarkar, S. S.; Ogawa, T.; Kitagawa, S. A New Dimension for Coordination Polymers and Metal–Organic Frameworks: Towards Functional Glasses and Liquids. *Angew. Chem. Int. Ed.* **2020**, *59* (17), 6652–6664. https://doi.org/10.1002/anie.201911384.

(57) Ou, L.; Zhou, Y.; Wu, B.; Zhu, L. The Unusual Physicochemical Properties of Azulene and Azulene-Based Compounds. *Chin. Chem. Lett.* **2019**, *30* (11), 1903–1907.

https://doi.org/10.1016/j.cclet.2019.08.015.

(58) Juvenal, F.; Lei, H.; Schlachter, A.; Karsenti, P.-L. L.; Harvey, P. D. Ultrafast Photoinduced Electron Transfers in Platinum(II)-Anthraquinone Diimine Polymer/PCBM Films. *J. Phys. Chem. C* **2019**, *123* (9), 5289–5302. https://doi.org/10.1021/acs.jpcc.9b00334.

(59) Harvey, P. D. Organometallic and Coordination Polymers, and Linear and Star Oligomers Using the Trans-Pt(PR3)2(C≡C)2 Linker. *J. Inorg. Organomet. Polym. Mater.* **2017**, *27* (S1), 3–38. https://doi.org/10.1007/s10904-017-0673-y.

For Table of Contents Only

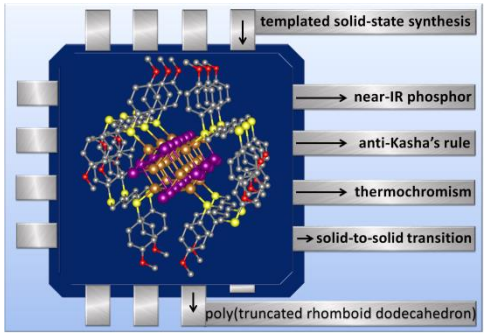

Synopsis

Upon thermal elimination of the coordinated MeCN ligands, the quasi-preassembled 1D-$[Cu_4I_4(\mathbf{L1})(MeCN)_2]_n$ crystal converts into the compact 3D-$[Cu_8I_8(\mathbf{L1})_2]_n$ material (**L1** = $ArS(CH_2)_4SAr$; Ar = 4-C_6H_4OMe). The structure consists of parallel and unprecedented fused 1D-poly(truncated rhomboid dodecahedron) interconnected by **L1**s. This material emits quite unexpectedly in the near-IR region at 298 K, but in the blue region at 77K, rendering it strongly thermochromic.